© 2018. Published by The Company of Biologists Ltd | Development (2018) 145, dev156315. doi:10.1242/dev.156315

STEM CELLS AND REGENERATION

RESEARCH ARTICLE

Direct control of somatic stem cell proliferation factors by the *Drosophila* testis stem cell niche

Eugene A. Albert[1,‡], Olga A. Puretskaia[1,‡], Nadezhda V. Terekhanova[2,3,4], Anastasia Labudina[1] and Christian Bökel[1,*,§]

ABSTRACT

Niches have traditionally been characterised as signalling microenvironments that allow stem cells to maintain their fate. This definition implicitly assumes that the various niche signals are integrated towards a binary fate decision between stemness and differentiation. However, observations in multiple systems have demonstrated that stem cell properties, such as proliferation and self-renewal, can be uncoupled at the level of niche signalling input, which is incompatible with this simplified view. We have studied the role of the transcriptional regulator Zfh1, a shared target of the Hedgehog and Jak/Stat niche signalling pathways, in the somatic stem cells of the *Drosophila* testis. We found that Zfh1 binds and downregulates *salvador* and *kibra*, two tumour suppressor genes of the Hippo/Wts/Yki pathway, thereby restricting Yki activation and proliferation to the Zfh1^{+} stem cells. These observations provide an unbroken link from niche signal input to an individual aspect of stem cell behaviour that does not, at any step, involve a fate decision. We discuss the relevance of these findings for an overall concept of stemness and niche function.

KEY WORDS: DamID, *kibra*, *salvador*, Stem cell niche, Zfh1, *Drosophila*

INTRODUCTION

Stem cell proliferation and maintenance are typically regulated by niches: signalling microenvironments within tissues that allow resident stem cells to fulfil their functions (Scadden, 2014). Since the first niches were characterised at the molecular level in the *Drosophila* ovary (Xie and Spradling, 2000) and testis (Kiger et al., 2001; Tulina and Matunis, 2001), niche-based regulation of stem cells has largely been discussed using a conceptual framework that considers stemness and differentiation as alternative outcomes of a cell fate decision. Niches were accordingly seen as a means by which the organism can influence this binary decision (Fuller and Spradling, 2007). However, this simplified model is at odds with recent observations in various model systems, including again the *Drosophila* gonadal stem cell niches. For example, stem cell proliferation and self-renewal in the fly testis were shown to be genetically separable at the level of Hedgehog (Hh) signalling input to the niche (Amoyel et al., 2013; Michel et al., 2012). Similarly, experimentally altering MAPK activity can uncouple stem cell self-renewal from the regulation of stem cell competitiveness (Amoyel et al., 2016a; Singh et al., 2016). These observations raise fundamental questions about the nature of stemness and the function of niches.

The *Drosophila* testis offers an excellent model system with which to address such issues. At the tip of the testis, two types of stem cells, the germline stem cells (GSCs) and the somatic cyst stem cells (CySCs), surround a group of postmitotic somatic niche cells termed the 'hub'. These hub cells provide multiple niche signals regulating both stem cell pools (Fig. 1A). In the somatic lineage, the CySCs are the only dividing cells, giving rise to differentiating cyst cells (CyCs) that exit the niche with the developing germline clusters (Losick et al., 2011). CySC maintenance and proliferation require niche signals by Unpaired (Upd) (Leatherman and Dinardo, 2008) and Hh (Amoyel et al., 2013; Michel et al., 2012). Both ligands are produced by the hub and activate the Jak/Stat and Smoothened signalling cascades, respectively, within the CySCs. Even though the two pathways each have multiple and specific targets, they converge on the large zinc-finger and homeodomain-containing transcription factor Zfh1 (Fortini et al., 1991). Zfh1 marks the somatic CySC pool within the testis and is absent from differentiated CyCs (Leatherman and Dinardo, 2008) (Fig. 1B). Similar to clonal inactivation of either Hh or Upd signalling, removal of their shared target *zfh1* leads to the loss of the mutant CySCs from the stem cell pool by differentiation (Amoyel et al., 2013; Leatherman and Dinardo, 2008; Michel et al., 2012). Zfh1 is thus required for CySC stemness.

It has been proposed that Zfh1 expression is also sufficient for CySC proliferation and self-renewal (Leatherman and Dinardo, 2008). However, the evidence for this is less clear: Upd overexpression or Jak/Stat pathway overactivation causes the proliferation of Zfh1^{+} CySC-like cells (Leatherman and Dinardo, 2008) (Fig. 1C) that retain some stem cell characteristics such as proliferation (Leatherman and Dinardo, 2008), but also acquire certain niche properties, including the expression of BMP ligands (Leatherman and Dinardo, 2010). This renders them able to recruit GSCs, a niche activity endogenously restricted to the hub (Inaba et al., 2015; Kawase et al., 2004; Michel et al., 2011), resulting in proliferating mixed lineage tumours. Prolonged overexpression of Zfh1 indeed causes a similar phenotype. However, whereas increased CySC proliferation in response to Zfh1 overexpression is rapidly detectable, tumour formation becomes observable only after weeks of overexpression (Leatherman and Dinardo, 2008), suggesting that additional regulatory events or signalling inputs must be involved.

Furthermore, overactivation of the Hh pathway also upregulates Zfh1 expression and causes accelerated proliferation of the mutant clones (Amoyel et al., 2013; Michel et al., 2012). However, despite

[1]Centre for Regenerative Therapies Dresden, Technical University Dresden, Fetscherstraße 105, 01307 Dresden, Germany. [2]Sector for Molecular Evolution, Institute for Information Transmission Problems of the RAS (Kharkevich Institute), Moscow 127994, Russia. [3]N. K. Koltsov Institute of Developmental Biology of the RAS, Moscow 119334, Russia. [4]Laboratory of Molecular Genetics, Russian Federal Research Institute of Fisheries and Oceanography, Moscow 107140, Russia.
*Present address: Department of Biology, Philipps-Universität Marburg, Karl-von-Frisch-Straße 8, 35043 Marburg, Germany.
‡These authors contributed equally to this work

§Author for correspondence (christian.boekel@biologie.uni-marburg.de)

C.B., 0000-0001-6603-6557

Received 20 June 2017; Accepted 6 July 2018

Development (2018) 145, dev156315. doi:10.1242/dev.156315

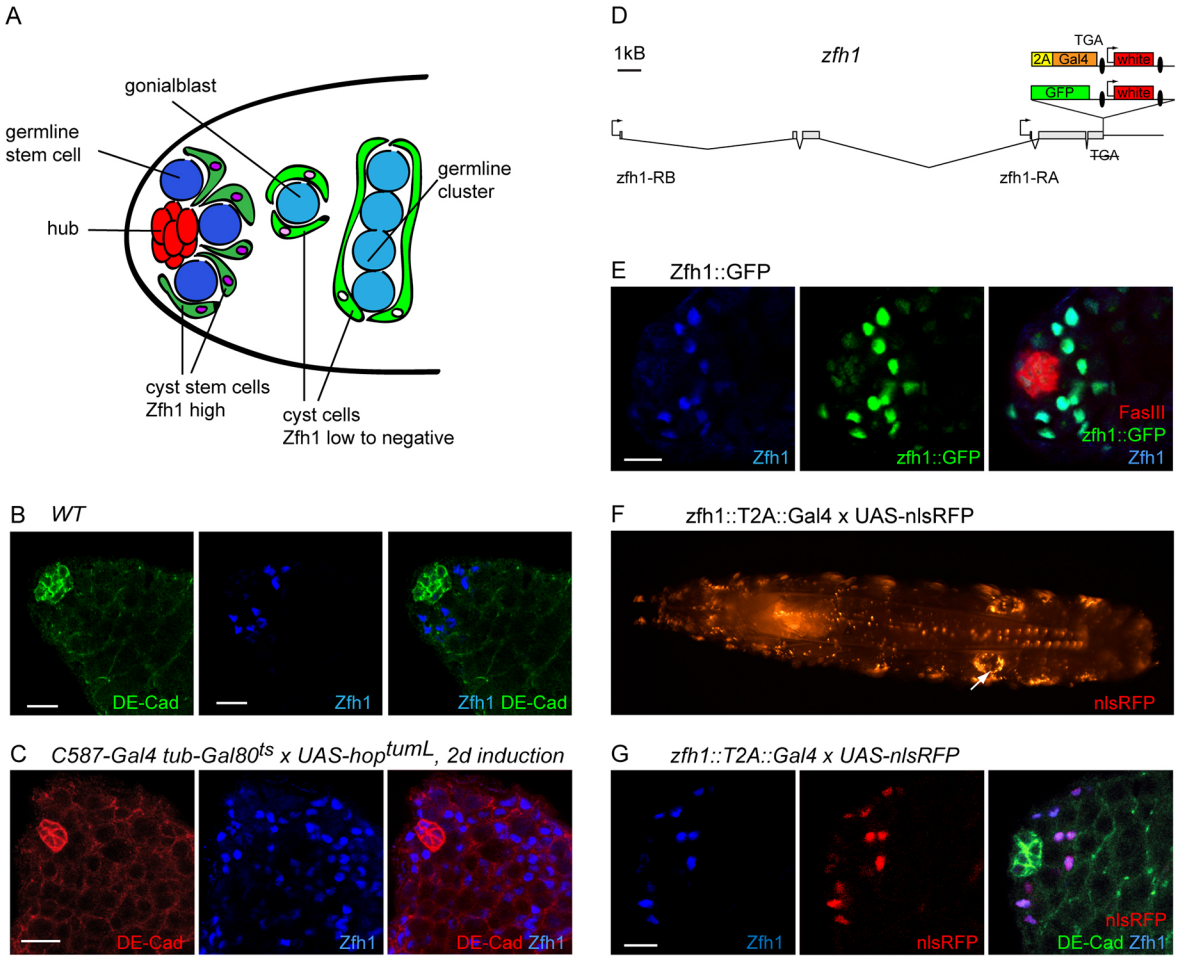

Fig. 1. Endogenous Zfh1 expression and Crispr/Cas9-generated reagents. (A) Schematic of the stem cell niche of the *Drosophila* testis tip. Zfh1 (magenta) marks the nuclei of the CySCs and, at lower levels, their immediate progeny. (B) CySCs are recognised by their Zfh1^{+} nuclei (blue) and their position adjacent to the hub (identified by strong DE-Cad expression, green). (C) Zfh1^{+} cells (blue) expand following a 2D pulse of the constitutively active Jak kinase Hop^{tuml}. Hub and CyC outlines are marked by DE-Cad (red). (D) Schematic of the Zfh1 locus, and C-terminal GFP and T2A-Gal4 fusions. Small ellipses indicate loxP sites flanking the white^{+} transgenesis marker. (E) Zfh1::GFP (green) colocalises with Zfh1 immunostaining (blue) in the vicinity of the hub (FasIII, red). (F,G) nlsRFP expression under control of zfh1::T2A::Gal4. In the larva, RFP is expressed in multiple tissues, including the testis (arrow) (F). In the adult testis, nlsRFP (red) coincides with Zfh1 protein (blue) labelling the CySCs abutting the hub (DE-Cad, green) (G). Scale bars: 10 µm.

initially expressing high levels of Zfh1, the affected cells retain the ability and propensity to differentiate (Amoyel et al., 2013; Michel et al., 2012), again suggesting that Zfh1 expression alone is insufficient for CySC fate.

We therefore hypothesised that a core role of Zfh1 is to promote CySC proliferation in response to either niche signal, and decided to identify Zfh1 target genes by mapping its binding sites in the CySCs using an *in vivo* DNA adenine methyltransferase identification (DamID) approach (Southall et al., 2013).

Here we report that: (1) Zfh1 binds to the putative control regions of multiple genes encoding upstream components of the Hippo/Warts/Yki signalling cascade, including the tumour suppressors *salvador* (*sav*) and *kibra*; (2) Zfh1 *in vivo* partially suppresses the transcription of these two genes; and (3) activation of Yki, which is necessary and sufficient for stem cell proliferation, is endogenously restricted to the Zfh1^{+} CySCs.

Niche signal input can thus directly be linked with transcriptional regulation of proliferation-associated genes, and none of the intervening steps constitutes a cell fate decision establishing stemness. We discuss the implications of these and other recent results for the overall concept of stemness, and propose an alternative model of niche function, whereby multiple niche signals directly and independently 'micromanage' distinct subsets of stem cell behaviour.

RESULTS

C-terminally tagged Zfh1 fusion proteins are functional

Visualisation of expression patterns by GFP reporters, and temporally and spatially controlled expression using the Gal4 system, are key elements of the *Drosophila* toolbox. The *zfh1* locus possesses two transcription starts, separated by about 17 kb. The respective transcripts are spliced to common 3′ exons (Fig. 1D), giving rise to two isoforms that are both expressed in the testis (Fig. S1). The first, *zfh1-RA*, encodes a 747 amino acid protein containing seven C2H2 zinc fingers and a central homeodomain, whereas the 1045 amino acid protein, encoded by *zfh1-RB*, contains two additional N-terminal zinc fingers and a polyQ region. We therefore targeted GFP to the common C terminus of both isoforms (Fig. 1D) by Crispr/Cas9-mediated recombination (Gratz et al., 2014; Port et al., 2014). The resulting zfh1::GFP knock-in lines were homozygous, viable and fertile. Zfh1::GFP marks the nuclei of somatic cells in the vicinity of the hub (32.7±4.2 GFP^{+} cells/testis,

Development (2018) 145, dev156315. doi:10.1242/dev.156315

n=20 testes), coinciding with the expression of endogenous Zfh1 (94.3±7.3% GFP and anti-Zfh1 double positive, *n*=20) (Fig. 1E).

To generate a driver line that captures expression of both isoforms, we fused Gal4 to the Zfh1 C-terminus via a co-translationally separating T2A peptide (Szymczak et al., 2004) (Fig. 1D). The zfh1::T2A::Gal4 knock-in flies were subviable in the homozygous state (~60% of expected adults hatching) and largely male sterile. Viability improved to Mendelian ratios and fertility recovered when the w^+ transgenesis marker was excised. In the larva, zfh1::T2A::Gal4-driven expression of nls-RFP encompassed multiple tissues in which Zfh1 is present (Broihier et al., 1998; Lai et al., 1991), including, for example, musculature, heart, nervous system, haemocytes and gonads (Fig. 1F). In the adult testis, RFP expression under control of zfh1::T2A::Gal4 was confined to the endogenously Zfh1$^+$ CySCs (Fig. 1G), demonstrating that the knock-in line can direct transgene expression to our cells of interest.

Zfh1 can therefore, in principle, tolerate C-terminal fusions. As the existing upstream activating sequence (UAS) constructs (Postigo and Dean, 1999) are based on *zfh1-RB*, we opted for C-terminal modification of this isoform for the cDNA-based DamID constructs described below.

Zfh1-binding sites identified by DamID in S2 cells are enriched at active regulatory regions

To identify Zfh1 target sites in the genome, we chose a next-generation sequencing- (NGS) based DamID approach using the targeted DamID (TaDa) system (Southall et al., 2013). This uses an mCherry leader open reading frame (ORF) (LT3) to achieve the desired low expression levels of the Dam and Dam fusion proteins (Fig. S2A). We first validated this approach for Zfh1 in Schneider 2 (S2) cells that also endogenously express Zfh1 (Fig. S2B). We generated stably transfected, polyclonal S2 cell lines that expressed either LT3-Dam or LT3-Zfh1::Dam under the control of the metallothionein promoter. Applying the DamID_seq analysis pipeline (Marshall and Brand, 2015) to our samples flagged 1125 peaks (Fig. 2A, Table S1) associated with 1052 genes (association criterion distance between DamID peak and ORF <1 kb) based on two replica experiments [Pearson's product-moment correlation between replicates r=0.91 (Dam) and r=0.86 (Zfh1::Dam)] (Fig. 2B, Table S1). Using a resampling/permutation approach (Zhu et al., 2010), we found that the S2 Zfh1 DamID peaks exhibited significant overlap with Zfh1-binding sites that have previously been identified by ChIP-seq in Kc167 cells (Nègre et al., 2011) (*n*=134, permutation test, P<0.001). To visualise the significance of these observations, the experimentally observed number of overlaps was plotted together with the distribution of overlaps resulting from the randomised resampling (Fig. 2C). Significant overlap was also observed between the genes associated with the Zfh1 peaks in either cell type (*n*=179, χ^2-test, P<0.0001) (Fig. 2D). In addition, 70% of the Zfh1 DamID peaks we identified in S2 cells coincided with regions flagged as enhancers in the same cell type by STARR-seq (Arnold et al., 2013) (Fig. S2C), again significantly more than is expected by chance (*n*=785, permutation test, P<0.001) (Fig. 2E).

Finally, we assayed whether the genes associated with the Zfh1 DamID peaks were under Zfh1 transcriptional control. For this, we analysed the transcriptome of S2 cells overexpressing a version of Zfh1 that is unable to bind the transcriptional corepressor CtBP (Zfh1-CIDm) (Postigo and Dean, 1999). As Zfh1-CIDm is not a full dominant negative but is expected to inactivate only one of several modes of transcriptional regulation by Zfh1, as shown for its mammalian homologue ZEB1 (Gheldof et al., 2012), cells similarly overexpressing wild-type Zfh1 were chosen as the most closely matched control sample. Upon overexpression of Zfh1-CIDm, 230 out of all 1052 genes associated with Zfh1 DamID peaks (21.9%) exhibited the expected signature of transcriptional derepression (Fig. 2F,G). A comparable number, however, showed decreased transcription levels relative to Zfh1 wild-type control (161/1052; 15.3%) (Fig. 2G and Fig. S2D), whereas the majority of genes associated with a Zfh1 peak experienced no significant difference between the two samples (661/1052 genes; 62.8%) (Fig. 2G and Fig. S2E, Table S2). Importantly, the fraction of genes exhibiting differences in transcription between samples, regardless of direction, was significantly higher among genes associated with at least one Zfh1 peak than for the overall transcriptome (37.5% versus 9.3%, χ^2-test: P<0.0001) (Fig. 2H). Thus, the Zfh1 DamID peaks were enriched for Zfh1-dependent regulatory elements.

Identifying Zfh1 target genes *in vivo*

However, there was no way of predicting *a priori* which of the targets identified in cell culture may be relevant *in vivo*. We therefore decided to also map Zfh1-binding sites directly in the CySCs of the adult testis, and generated transgenic flies expressing Zfh1-Dam with the LT3 mCherry leader ORF under UAS control (UAS-LT3-zfh1::Dam) (Fig. S3A). To suppress transgene expression before induction, we recombined tub-Gal80^{ts} transgenes both onto the chromosomes carrying the UAS-LT3-Dam or UAS-LT3-zfh1::Dam insertions and onto the zfh1::T2A::Gal4 driver line. Following a 24 h pulse of transgene expression, DNA was then extracted from dissected testes.

Applying the same analysis as above uncovered 811 Zfh1 peaks (Fig. 3A, Table S3) present in both replicates [Pearson's product-moment correlation between replicates r=0.91 (Dam) and r=0.86 (Zfh1::Dam)], which already, in a first-pass inspection, included potential Zfh1 targets such as *eyes absent* (*eya*) or *shotgun* (Le Bras and Van Doren, 2006; Leatherman and Dinardo, 2008) (Fig. 3B). Of these sites, 377 (46%) were also occupied in S2 cells (Fig. 3C), corresponding to 420 of the 968 genes associated with Zfh1 in CySCs (43%) (Fig. 3D, Table S3). Of the CySC zfh1 DamID peaks, 18% coincided with enhancers identified by STARR-seq in cultured ovarian somatic cells (OSCs) (Arnold et al., 2013), mesodermal cells developmentally related to the CySCs (Fig. 3E,F). This was, again, significantly more than expected by chance (*n*=150, permutation test, P<0.001). Significant overlap was also observed between the CySC Zfh1 DamID peaks and the Kc167 Zfh1 ChIP peaks (*n*=67, permutation test, P<0.001), and between the associated genes (*n*=113, χ^2-test, P<0.001) (Fig. S3B,C). Finally, Gene Ontology (GO) analysis using Panther GO-Slim (Mi et al., 2016) revealed that a limited number of biological processes (7 of 222 terms) was overrepresented among the putative Zfh1 target genes (Fig. 3G and Fig. S3D). The GO term 'signal transduction' immediately raised our interest as a potential link to CySC proliferation.

Zfh1 binds at or near genes encoding members of the Hippo signalling cascade

We were therefore intrigued by a cluster of hits in or near genes encoding components of the Hippo (Hpo) signalling cascade. This pathway is associated with cell growth, proliferation and survival (Enderle and McNeill, 2013; Irvine and Harvey, 2015; Meng et al., 2016), and is necessary and sufficient for CySC proliferation (Amoyel et al., 2014). However, it remains unknown whether, or how, its activity is regulated by niche signals.

The Hippo signalling cascade consists of a core of two serine/threonine kinases, Hpo and Warts (Wts), that phosphorylates, and thus inactivates, the effector transcription factor Yorkie (Yki), with

Development (2018) 145, dev156315. doi:10.1242/dev.156315

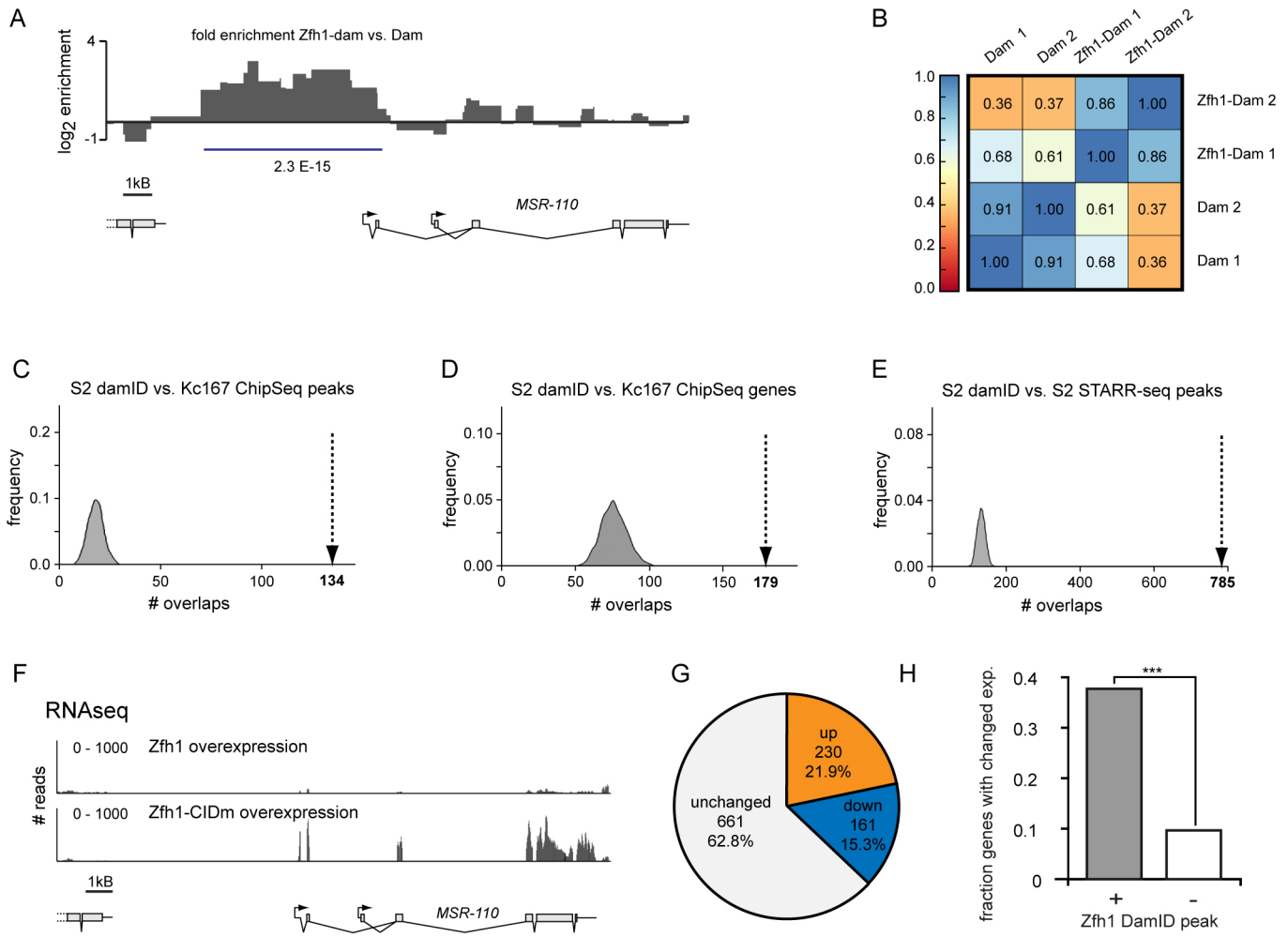

Fig. 2. Zfh1 DamID in S2 cells. (A) NGS reads from a Zfh1-Dam sample are enriched relative to a Dam-only control near the MSR-110 distal transcription start (log_2 of ratio plotted versus genome position; peak as called by DamID_seq, blue line; false discovery rate indicated). (B) Pearson's correlation between S2 cell Zfh1-Dam and Dam control samples, two biological replicates. (C-E) Overlap of Zfh1 DamID peaks in S2 cells or their respective associated genes, with datasets from ChIP-seq and STARR-seq experiments. Zfh1 DamID peaks in S2 cells show significant overlap with Zfh1 ChIP peaks in Kc167 cells (P<0.001, permutation test) (C). Genes associated with Zfh1 DamID peaks in S2 cells and Zfh1 ChIP peaks in Kc167 cells show significant overlap (P<0.001, χ^2-test) (D). Zfh1 DamID peaks in S2 cells overlap with enhancer regions identified by STARR-seq (P<0.001, permutation test) (E). Distribution of overlaps from 1000 simulated resamplings of the Zfh1 peaks plotted against frequency; dashed arrows indicate experimentally observed values. (F-H) Transcriptional differences between S2 cells overexpressing either wild-type Zfh1 or a Zfh1 construct unable to bind CtBP (zfh1-CIDm). Number of RNA-seq reads plotted against genomic position reveals transcriptional derepression of the *MSR-110* gene in response to Zfh1-CIDm (F). Response to zfh1-CIDm overexpression relative to Zfh1 control by genes associated with a Zfh1 DamID peak (G). Genes associated with a Zfh1 DamID peak are significantly more likely than other genes to exhibit differences in transcription levels between Zfh1 and Zfh1-CIDm samples (***P<0.001, χ^2-test) (H).

the help of the associated adaptor proteins Sav (Tapon et al., 2002) and Mob-as-tumour-suppressor (Mats), and scaffolding proteins such as Expanded (Ex), Kibra (Baumgartner et al., 2010; Genevet et al., 2010; Yu et al., 2010) and Merlin that recruit the complex to the plasma membrane. Inactivation of the upstream components or the kinase complex by physiological signals or by mutation allows Yki to promote target gene expression. In CySCs, we detected Zfh1 binding at or near the *kibra*, *sav* and *mats* genes (Fig. 3A and Fig. S4). In S2 cells, binding was also observed near *ex*, *pez*, *wts* and *scalloped* but not near *mats* (Fig. S4).

The ability of overexpressed Zfh1 to induce CySC proliferation depends on its function as a CtBP-dependent transcriptional repressor (Leatherman and Dinardo, 2008; Postigo and Dean, 1999). Upd and/or Hh niche signals produced by the hub could thus potentially activate Zfh1 expression locally, in adjacent somatic cells, which would in turn repress multiple Hpo pathway components, thereby activating Yki exclusively in the Zfh1$^+$ stem cells. Consistently, a transcriptional reporter for Yki activity (diap1-GFP4.3), in which a minimal Yki response element from the *diap1* gene drives expression of a nuclear GFP (Zhang et al., 2008), is in the adult testis, restricted to the Zfh1$^+$ CySCs (89±9% of all Zfh1$^+$ cells and 84±7% diap-GFP$^+$ cells double positive for both Zfh1 and diap-GFP) (Fig. 4A). Moreover, Zfh1 overexpression in the somatic lineage using the *traffic jam* (*tj*)-Gal4 driver expanded the region exhibiting Yki activation (Fig. 4B,C), and the associated increase in somatic cell count was sensitive to *yki* copy number (Fig. S5A,B). For the remaining experiments we focused on two of the putative target Zfh1 genes: *sav* and *kibra*.

Sav and Kibra limit CySC proliferation

We first confirmed that *kibra* and *sav* affected proliferation in the testis, as has previously been shown for *hpo* (Amoyel et al., 2014).

Development (2018) 145, dev156315. doi:10.1242/dev.156315

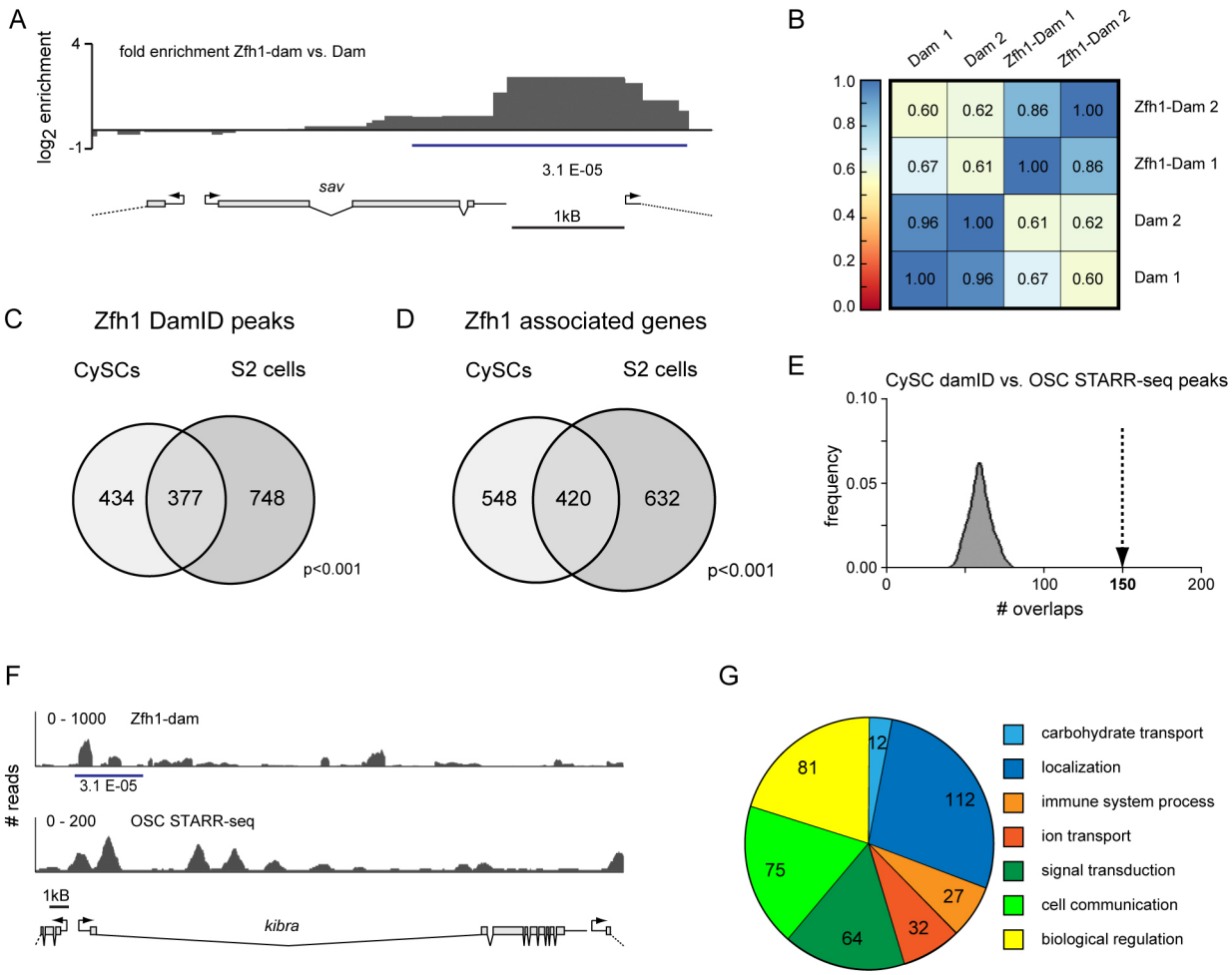

Fig. 3. *In vivo* Zfh1 DamID in CySC cells. (A) Zfh1 DamID reads are enriched near the 3′-UTR and downstream intergenic region of the *sav* locus (extent of DamID peak, blue line; false discovery rate indicated). (B) Pearson′s correlation between CySC *in vivo* DamID samples, two biological replicates. (C,D) Venn diagrams show that 46% of CySC DamID peaks (C) and 43% of the associated genes (D) are also recovered in S2 cells, significantly more than expected by chance (C, P<0.001, permutation test; D, P<0.001, χ^2-test). (E) CySC Zfh1 DamID peaks overlap with enhancer regions in ovarian somatic cells (P<0.001, permutation test). Dashed arrow indicates experimentally observed values. (F) Comparison of Zfh1 DamID peaks in CySCs with STARR-seq peaks in cultured ovarian stem cells for the *kibra* locus. (G) GO-slim terms enriched among Zfh1-associated genes.

Homozygous *kibra* clones rapidly expanded relative to controls (Fig. 4D,E). Bromodeoxyuridine (BrdU) labelling confirmed that this was caused by increased proliferation (Fig. S5C,D). Homozygosity for *kibra* did not block differentiation, as indicated by the expression of both the CySC marker Zfh1 and the CyC differentiation marker Eya (Fabrizio et al., 2003) in different mutant cells within the same testis (Fig. 4F). Consequently, both 3 and 5 days after clone induction (ACI) the fraction of Zfh1$^+$ cells did not differ between control and *kibra* mutant clones (Fig. 4G). The increased proliferation of the *kibra* mutant cells is thus uncoupled from their ability and propensity to differentiate. The effect of clonal inactivation of *sav* was less pronounced in the short term but was, as for *kibra*, readily detectable by increased long-term retention of the clones, reflecting a reduced rate of loss from the niche because of skewed neutral competition (Amoyel et al., 2014) (Fig. S5E,F).

Kibra is expressed in the somatic lineage and is downregulated by ectopic Zfh1 expression

We therefore wanted to know whether Kibra expression was reduced in the CySCs under physiological conditions. However, in the adult testis, Kibra antibody staining marks most strongly the spectrosomes and fusomes in the germline (Fig. 5A), even though the Hpo pathway does not regulate the proliferation of this lineage (Amoyel et al., 2014; Sun et al., 2008). In the soma, Kibra protein could, with confidence, only be observed in the hub, whereas the diffuse staining at the interface of germline and somatic cells could not be assigned to either lineage because of their tight apposition.

To assess *kibra* transcription in the testis, we therefore generated a construct containing *kibra* exons 5-9, C-terminally fused to a nuclear GFP via a T2A site. This construct was then targeted to a MiMIC landing site (MI13703) (Venken et al., 2011) inserted in the fourth intron of the *kibra* locus (Fig. 5B), resulting in viable and fertile kibra::T2A::GFPnls flies. Nuclear GFP expression clearly demonstrated *kibra* expression in both germline and soma. Within the somatic lineage, nuclear GFP immunofluorescence was strongest in the hub (184% of median GFP levels in CyCs) (Fig. 5C,D). A somewhat weaker signal was also visible in CySCs, identified here as cells abutting the hub and expressing the somatic nuclear marker Tj, and in recently differentiated CyCs (Tj$^+$ cells one tier further out) (Fig. 5C). Compared with the CyCs, median nuclear GFP levels in the CySC were reduced by 23% (Fig. 5D), consistent with the hypothesis that Zfh1 downregulates *kibra* transcription.

However, the presence of multiple Zfh1 DamID peaks near and within the *kibra* transcription unit (Fig. S4) meant that it was

Development (2018) 145, dev156315. doi:10.1242/dev.156315

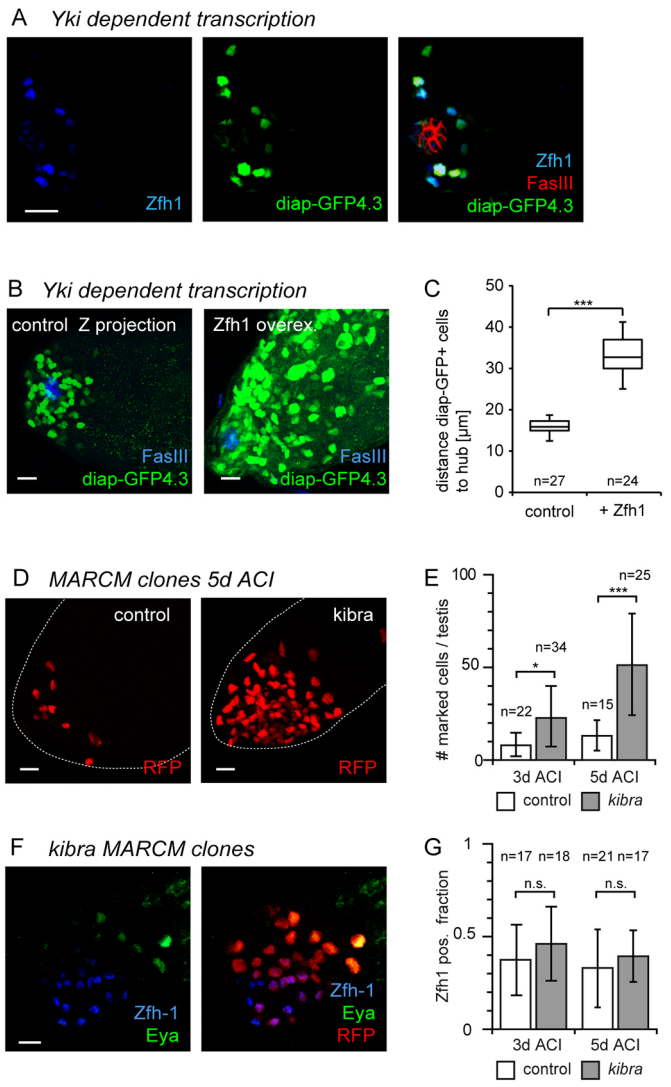

Fig. 4. The Hippo pathway controls CySC proliferation. (A) Activity of a transcriptional reporter (green) driving GFP expression from a Yki-dependent fragment of the diap1 promoter (diap-GFP4.3) is restricted to Zfh1$^+$ CySCs (blue). Hub marked by FasIII (red). (B) Zfh1 overexpression under tj-Gal4 control for 8d expands the population of cells with active Yki (green) to regions further from the hub (FasIII, blue). (C) Quantification of the average distance of diap-GFP4.3$^+$ cells to the hub in controls versus testes overexpressing Zfh1 under tj-Gal4 control for 8d. First and third quartile (box), median (horizontal line) and mean; whiskers, data range up to 1.5× interquartile distance; *n*, number of testes. (D) Homozygous *kibra* mutant MARCM clones (RFP, red) overproliferate relative to control clones. (E) Quantification of homozygous *kibra* or control cells per testis (*n*, number of testes) at 3 days and 5 days ACI. (F) *kibra* mutant cells (RFP, red) within the same testis overlap both with the stem cell marker Zfh1 (blue) and the differentiation marker Eya (green). (G) *kibra* and control clones do not differ in the fraction of Zfh1$^+$ clonal cells. Data are mean±s.d. **P*<0.05, ****P*<0.01 (*t*-test). *n*, number of testes; n.s., not significant. Scale bars: 10 µm.

impractical to test directly whether *kibra* expression in the CySCs is downregulated by endogenous Zfh1 by deleting the corresponding binding sites. Conversely, clonal inactivation of Zfh1 causes the rapid exclusion of the mutant cells from the stem cell compartment (Leatherman and Dinardo, 2008), making it impossible to decide whether a possible effect on *kibra* expression was caused directly by the absence of Zfh1, or was a consequence of differentiation.

We therefore turned to mosaic expression of Zfh1 in hub cells, which endogenously express Kibra but not Zfh1. This allowed us to test *in vivo* whether Zfh1 expression was sufficient to suppress *kibra* transcription activated by other transcription factors. In line with the observations on the Zfh1$^+$ CySCs and their Zfh1$^-$ progeny, GFP levels in hub cell nuclei that overexpressed Zfh1 were reduced by 15% relative to their non-overexpressing neighbours (Fig. 5E,F).

Sav expression is sensitive to endogenous Zfh1

Unlike *kibra*, the *sav* locus possesses only a single Zfh1 DamID peak, located 3′ of the coding region (Fig. 3A). To test whether endogenous Zfh1 expression is sufficient for downregulating its target genes, we therefore concentrated on Sav, using a series of GFP-based transcriptional reporter constructs inserted in the attB2 landing site by ΦC31-mediated recombination (Fig. 6A).

For this, we isolated a genomic fragment spanning the *sav* genomic region, including parts of the flanking transcription units and the entire Zfh1 DamID peak. As for Kibra, we tagged Sav with T2A::GFPnls. Nuclear GFP from this sav::T2A::GFPnls reporter was expressed in the germline, with a weaker signal in the somatic CySCs and CyCs but no expression in the hub (Fig. 6B). As derepression of *sav* in the CyCs might negatively affect stem cell maintenance, we next deleted the Sav-coding region and T2A cassette, generating a pure transcriptional reporter line (Fig. 6A). The GFP signal of this GFPnls-full length construct was indistinguishable from that of the sav::T2A:GFPnls reporter, confirming that the Sav-coding region does not include essential *cis*-regulatory regions (Fig. 6B,C).

DamID resolution is intrinsically limited by the separation of the GATC target sites, 1063 bp in the case of the *sav* Zfh1 DamID peak. This region contains a short motif with high similarity (10 bp out of 12 bp identical) to the Zfh1 homeodomain-binding site within the *eve* mesodermal enhancer (Su et al., 1999), which resembles the conserved *Rhodopsin* Core Sequence I (RCSI) homeodomain-binding motif originally used for cloning *zfh1* (Fortini et al., 1991) (Fig. 6A). Sites corresponding to the degenerate RCSI-like sequence CTAATYRRNTT (Su et al., 1999) were indeed significantly enriched in Zfh1 DamID peaks from both S2 cells and CySCs [S2 cells: PWMEnrich raw score 1.377; *P*=8.06 E-11; CySCs: raw score 1.421; *P*=1.377 E-07; bioconductor.org/packages/release/bioc/html/PWMEnrich.html (doi:10.18129/B9.bioc.PWMEnrich)].

We next removed the central one-third of the *sav*/*CG17119* intergenic region that includes the single RCSI-like sequence motif within the Zfh1 DamID peak (GFPnls-ΔNsiPst). In the final construct, we selectively deleted this putative Zfh1-binding site (GFPnls-ΔRCSI) (Fig. 6A).

We then quantified relative GFP fluorescence in CySC and adjacent CyC nuclei for all four reporter lines (Fig. 6B-F). For both the sav::T2A::GFPnls and the GFP-full length constructs (Fig. 6B,C), GFP fluorescence was ∼20% lower in the endogenously Zfh1$^+$ CySCs (again identified by position and Tj immunostaining) than in their differentiating CyC neighbours (Fig. 6F). This difference was abolished for both constructs carrying the deletions within the Zfh1 DamID peak (GFPnls-ΔNsiPst and GFPnls-ΔRCSI) (Fig. 6D-F), confirming that the RCSI-like motif is the *cis*-acting element responsible for downregulation of *sav* expression in the Zfh1$^+$ CySCs.

To test whether the observed partial reduction in both Sav and Kibra levels could together be sufficient for triggering CySC proliferation, we quantified the number of Zfh1$^+$ CySCs in testes of *sav* and *kibra* single or double heterozygous flies versus controls. (Fig. 6G). However, there were no significant differences in CySC number per testis, suggesting that these stem cells either do not proliferate more strongly when the dose of both Kibra and Sav is

Development (2018) 145, dev156315. doi:10.1242/dev.156315

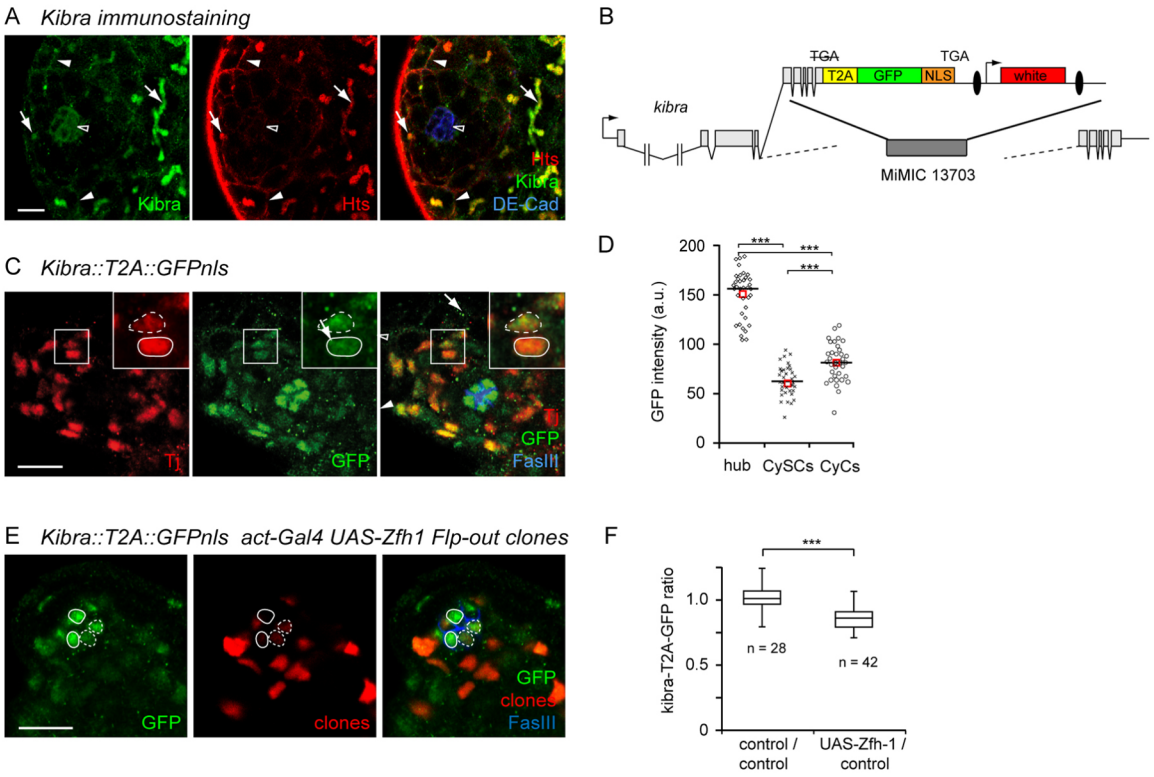

Fig. 5. Kibra expression in the testis. (A) Kibra immunostaining (green) is detectable in the somatic hub cells (DE-Cad, blue, hollow arrowhead) as well in punctate structures corresponding to spectrosomes and fusomes of the germline (Hts, red, arrows). Diffuse cortical Kibra staining around cell outlines (solid arrowheads) cannot be assigned unambiguously to either lineage. (B) A kibra-T2A-GFPnls construct inserted into a MiMIC landing site preceding exon 5. Ellipses indicate loxP sites. (C-F) GFP immunostaining in the kibra-T2A-GFPnls reporter line. Nuclear GFP is visible both in the germline (large, diffusely stained nuclei) and the somatic lineage, with pronounced staining in the hub (FasIII, blue). Note reduced signal in CySC nuclei identified as Tj^+ (red) nuclei abutting the hub (solid outline in inset) relative to their CyC neighbours (dashed outline) (C). Quantification of GFP intensities in C for the different cell types, n=13 testes. Data are shown as individual data points, median (solid line) and mean (red square). ***P<0.01 (ANOVA) (D). Zfh1 overexpression in RFP marked Flp-out clones (red, dashed outline) in the hub (FasIII, blue) decreases nuclear GFP levels (green) relative to sibling cells (solid outline) (E). Ratio of GFP immunofluorescence between Zfh1-expressing and adjacent non-expressing nuclei or between controls. First and third quartile (box) and median (horizontal line); whiskers, data range up to 1.5× interquartile distance. ***P<0.01 (t-test) (F). Scale bars: 10 µm.

reduced, or that the overall size of the stem cell pool is also regulated by additional mechanisms. In addition, epistasis experiments between *zfh1* and *yki* were inconclusive: neither Zfh1 overexpression in *yki* mutant clones (Fig. S5G) nor expression of dominantly active, nonphosphorylatable Yki (YkiS168A) in *zfh1* mutant cells (Fig. S5H) was able to rescue the loss of the respective clones. Taken together, our observations show that: the DamID experiments successfully uncovered target genes that are regulated by Zfh1 in the adult testis; the regions flagged as Zfh1-binding peaks contain sequence elements conveying Zfh1 sensitivity; and Zfh1 downregulates transcription of Hpo pathway components, which may contribute to CySC proliferation and is consistent with the pattern of endogenous Yki activation.

DISCUSSION

Stemness and differentiation have long been treated as alternative outcomes of a binary cell fate decision made by a stem cell that would subsequently govern its behaviour (Fuller and Spradling, 2007). However, we, and others, had previously shown that experimental activation of the Hh pathway upregulates proliferation of somatic CySCs, but does not affect the differentiation propensity of the mutant clones (Amoyel et al., 2013; Michel et al., 2012). In contrast, overexpression of Upd instead drives the proliferation of stem cell-like cells that fail to differentiate, but partially acquire hub functions (Leatherman and Dinardo, 2008). Activation of MAPK signalling can uncouple stem cell self-renewal from the regulation of cell competition and adhesion to the niche (Amoyel et al., 2016a; Singh et al., 2016). Manipulation of either of these endogenously active signalling pathways thus impinges on overlapping, but distinct, subsets of stem cell properties. However, such partial alteration of stem cell behaviour should not be possible if niche signals became integrated into a decision between stemness and differentiation (Fig. 7A).

The results presented here provide a regulatory link between niche signal input and the transcription of genes involved in stem cell proliferation that does not involve any individual step that would be by itself sufficient for stemness. The Hh and Upd niche signals converge on Zfh1 (Amoyel et al., 2013; Leatherman and Dinardo, 2008; Michel et al., 2012), which we found to bind to multiple genes that encode regulators of the Hippo signalling cascade. For two of these genes, *sav* and *kibra*, we could show that this results in a partial suppression of transcription, as reflected by reduced reporter gene expression in endogenously $Zfh1^+$ CySCs. For *sav* we were able to identify a short putative homeodomain-binding motif within the Zfh1 DamID peak as the *cis*-acting sequence that is necessary to convey repression in endogenously $Zfh1^+$ cells. Conversely, Zfh1 mis-expression in the hub demonstrated that Zfh1 is, *in vivo*, sufficient to suppress *kibra* transcription driven by other, as yet unknown, transcriptional regulators. Even though both genes are downregulated in CySCs by

Development (2018) 145, dev156315. doi:10.1242/dev.156315

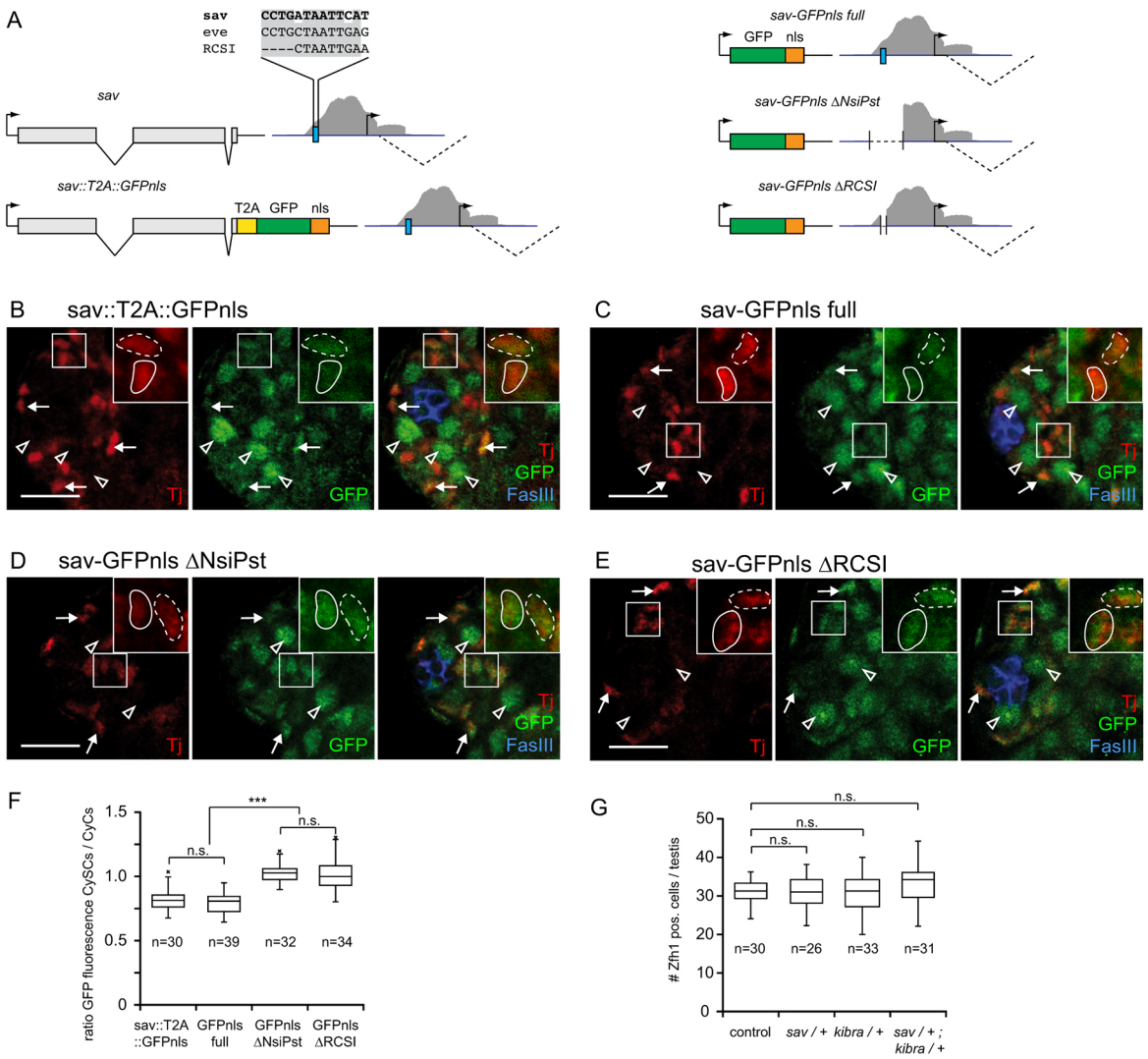

Fig. 6. Sav in the adult testis. (A) Organisation of the *sav* locus, the sav-T2A-GFPnls construct, and the sav::GFPnls transcriptional reporters. Blue line, extent of Zfh1 DamID peak (grey shading); blue box, RCSI-like putative Zfh1-binding site. Sequences from *sav*, the *eve* Zfh1-binding site and the original RCSI sequence are indicated. (B-E) GFP immunofluorescence from the *sav* reporter constructs. Note GFP signal (green) in the large germline nuclei (arrowheads) and smaller somatic nuclei (arrows, marked by Tj, red); hub marked by FasIII (blue). In the sav-T2A-GFPnls fusion construct (B) and the sav::GFP_full transcriptional reporter (C), the GFP signals in CySC nuclei (identified by proximity to hub, solid outline in inset) are reduced relative to the adjacent CyC nuclei (dashed outlines in inset). In sav::GFPnls_ΔNsiPst (D) and sav::GFPnls_ΔRCSI (E) transgenic flies, the difference in GFP intensity between CySC and CyC nuclei vanishes. (F) Quantification of the GFP intensity ratios between pairs of adjacent CySC and CyC nuclei for B-E. (G) Quantification of Zfh1^{+} cells for controls and *sav* and *kibra* single and double heterozygous males. First and third quartile (box) and median (horizontal line); whiskers indicate data range up to 1.5× interquartile distance. Outliers are marked individually. ***P<0.01 (ANOVA); *n*, number of testes; n.s., not significant. Scale bars: 10 µm.

no more than 25%, Yki activation in the testis is tightly restricted to the Zfh1^{+} stem cells. As the loss of one copy of any individual Hpo pathway gene, or even double heterozygosity for *kibra* and *sav*, has no obvious proliferative phenotype, we postulate that Yki activity is controlled cooperatively through the modulation of multiple regulators that may, in addition, be influenced by multiple upstream stimuli. Although *kibra* and *sav* appear to be transcriptionally controlled by niche signalling via Zfh1, the upstream Hpo pathway regulator Merlin has recently been implicated in regulating CySC proliferation in response to cell adhesion (Inaba et al., 2017). Surprisingly, in the ovary Hh regulates Hpo signalling through transcriptional control of Yki (Huang and Kalderon, 2014). We currently have no explanation for why the male and female niches should make use of the same molecular players but follow a different regulatory logic.

Generalising from this direct link between niche signals and the genes involved in proliferation, and considering other examples in which different aspects of stem cell behaviour can be uncoupled at the level of niche signal input (Amoyel et al., 2016a; Leatherman and Dinardo, 2008; Singh et al., 2016), we suggest that the function of the niche is to directly instruct competent cells to execute specific stem cell behaviours. ‘Stemness’ would thus become an operational description given to any cell instructed to self-renew and produce offspring that differentiate, without having to invoke a cell fate decision. We would like to propose the term ‘micromanagement’ for this mode of niche-mediated stem cell regulation (Fig. 7B).

Of course, this model comes with several caveats. First, the somatic CySCs of the fly testis or the stem cells of the mammalian intestinal epithelium (Beumer and Clevers, 2016) may represent one extreme within a continuum of stem cell/niche systems that differ in their

Development (2018) 145, dev156315. doi:10.1242/dev.156315

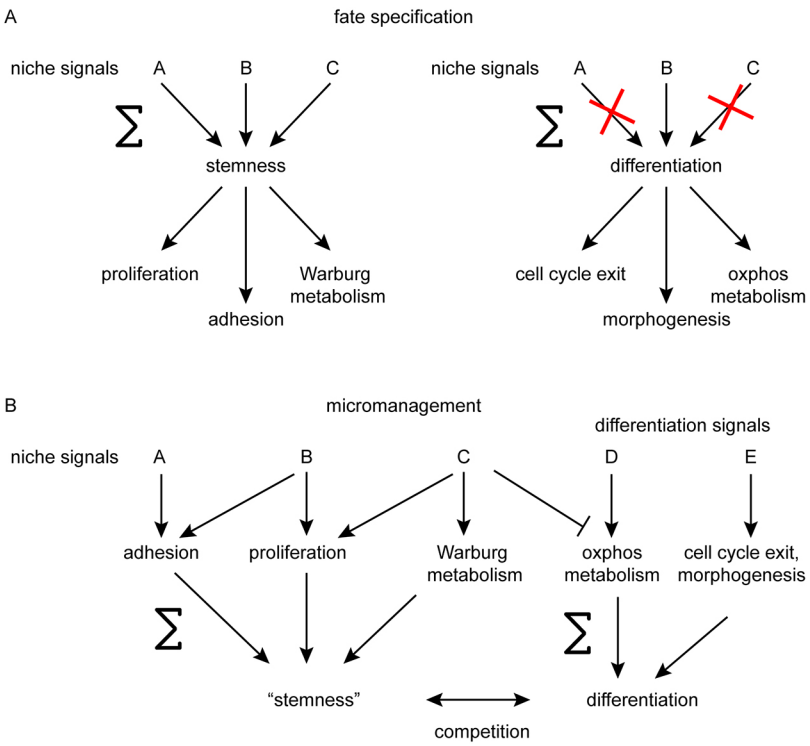

Fig. 7. Models of stemness and niche function. (A) According to the standard model, multiple niche signals are integrated into a decision to adopt stem cell fate. Differentiation is the default response when some of these signals are absent. Explaining why increasing one particular niche signal can impinge on only one or on a few aspects of stem cell behaviour, thus uncoupling these traits, is not straightforward. (B) Under the proposed micromanagement model, niche signals continuously control genetically separable subsets of stem cell behavioural output. Stemness becomes a compound phenotype rather than a binary cell fate. Differentiation is similarly specified by additional signals that include cues from the intense cell competition in the niche.

relative contributions of fate specification and micromanagement. The mammalian haematopoietic system, which has guided much of our thought about stemness and niches (Scadden, 2014), and indeed the *Drosophila* germline stem cells, which are maintained primarily through suppression of the differentiation factor Bam by a hub-derived BMP niche signal (Chen and McKearin, 2003; Kawase et al., 2004), may represent the other end of the spectrum.

Second, the competence of a cell to respond to a given niche microenvironment clearly depends on cell fate decisions along its developmental trajectory. Unlike the CySC/CyC lineage, the muscle sheath of the testis does not respond to Upd or Hh overexpression by proliferating, even though both cell types are of mesodermal origin.

Third, the micromanagement model we propose will still be a truncation of the true regulatory network. For example, we already know that different aspects of stem cell activity in the testis are coupled by competition (Amoyel et al., 2016a; Issigonis et al., 2009; Michel et al., 2012; Singh et al., 2016), making it difficult to analyse loss-of-function conditions, as affected cells are eliminated by differentiation regardless of the actual function of the affected pathway. In addition, the subsets of stem cell behaviours controlled by different niche signals may overlap, and any individual signal can control multiple aspects of stemness. For example, Upd not only cooperates with Hh to promote CySC proliferation through Zfh1, but independently ensures male-specific development of the somatic lineage through Chinmo (Flaherty et al., 2010; Ma et al., 2014).

Interestingly, a corresponding argument may be made for cyst cell differentiation. Recent work from several labs suggests that it, too, appears to be a highly regulated process involving detailed instructions through several niche-like signals, rather than only reflecting a general loss of stemness-maintaining factors (Amoyel et al., 2016b; Hudson et al., 2013).

Even Zfh1 itself is likely to control additional aspects of stemness. Hpo pathway components account for only a small fraction of the many hundred potential target genes we identified in the CySCs. For example, we also found Zfh1 peaks near multiple genes involved in glucose and energy metabolism, with carbohydrate transport appearing as a significantly enriched GO term. This invites the speculation that a potential, Warburg-like stem cell metabolic state (Chandel et al., 2016) may also be the outcome of detailed continuous regulation by the niche rather than a consequence of stem cell fate. Furthermore, such additional functions may explain why Yki activation is insufficient to rescue clonal loss of Zfh1.

Finally, under our micromanagement model, the minimal unit of stemness is a stem cell together with its niche. Obviously, this can only hold true for tissue-resident stem cells that are actually integrated with a niche, but may not apply to embryonic stem cells that are, at least *in vitro*, able to retain their stem cell properties in the absence of a complex signalling microenvironment.

MATERIALS AND METHODS

Fly stocks and transgenic lines

The following fly stocks were obtained from the Bloomington Drosophila Stock Center:

w;UAS-zfh1,
w;;UAS-RedStinger,
w;;FRT82B w^{+}90E,
w;Sco/CyO;tub-GAL80^{ts},
y w;MiMIC kibra^{MI13703},
y w;;Act5C>CD2Y>GAL4
and y sc v nos-phiC31Int;;attP2.

The following stocks were graciously provided by our colleagues: UAS-Hop^{tumL} (Bruce Edgar, University of Utah, Salt Lake City, UT, USA); y w vasa-Cas9/FM7c (Anne Morbach, Max Planck Institute of Molecular Cell Biology and Genetics, Dresden, Germany); UAS-LT3-Dam (Andrea Brand, University of Cambridge, UK); tj Gal4 Gal80^{ts} (Doug Allan, University of British Columbia, Vancouver, Canada); y w;Sp/CyO, y^{+};FRT82 kibra^{1}/TM6B, Tb, Hu; y w;Sp/CyO,y^{+};diap1-GFP4.3/TM6B, Tb; w;FRTD 42D yki^{B5}/CyO (Hugo Stocker, Institute of Molecular Systems Biology, ETH, Zürich, Switzerland); and FRT 82B sav^{3}/TM3 Sb (Florence Janody, Instituto Gulbenkian de Ciencia, Oeiras, Portugal; Nic Tapon, Francis Crick Institute, London, UK).

Development (2018) 145, dev156315. doi:10.1242/dev.156315

MARCM clones (Lee and Luo, 1999) were generated by crossing FRT males with w hs-FLP C587-Gal4 UAS-RedStinger virgins carrying the appropriate tub-Gal80 FRT chromosomes, and heat shocking adult males for 1 h at 37°C. The zfh1::GFP and zfh1::T2A::Gal4 lines were generated by co-injecting two pU6-BbsI-gRNA plasmids (Gratz et al., 2014) (Addgene, 45946) with a pRK2-derived plasmid (Huang et al., 2008) containing the transgene sequence, 1 kb homology arms and a w^+ selection marker into y w vasa-Cas9/FM7c.

The kibra::T2A::GFP line was generated by injecting a pBSKS-attB1_2SASD-0 plasmid (Frank Schnorrer, University of Marseille, France) containing kibra exons 5 to 9 fused to T2A-GFPnls into nos-phiC31Int;MiMIC kibra^{MI13703}. The Sav reporter constructs were generated by fusing a T2A::GFPnls cassette to the Sav C-terminus. The Sav-coding region and the 3′ UTR segments were then excised and deletions introduced to the Zfh1 DamID peak. For UAS-LT3-zfh1::Dam the zfh1-RB ORF (Korneel Hens, University of Oxford, UK) was inserted into pUAST-attB-LT3-Dam (Andrea Brand). Plasmid sequences are provided in the Supplementary Information.

Antibodies and immunohistochemistry

Testes were stained as previously described (Michel et al., 2011), incorporating a 1 h incubation with 1% Triton X-100 following fixation. The following antisera were used: rat anti-DECadherin (Developmental Studies Hybridoma Bank, DCAD2, 1:100), mouse anti-Eya (Developmental Studies Hybridoma Bank, eya10H6, 1:20), mouse anti-FasIII (Developmental Studies Hybridoma Bank, 7G10, 1:100), rabbit anti-GFP (Clontech, 632592, 1:500), rabbit anti-Kibra (Nic Tapon, 1:200), rat anti-Tj (Dorothea Godt, University of Toronto, Canada, 1:250), rabbit anti-vasa (Paul Lasko, McGill University, Montreal, Canada, 1:5000), rabbit anti-Zfh1 (Ruth Lehmann, NYU School of Medicine, NY, USA, 1:4000). Alexa-488, -568 or -633 secondary antibodies were used (Invitrogen, A-11001, A-11004, A-21050, A-11077, A-21094, A-11034, A-11036 and A-21071, 1:500).

BrdU labelling

Flies were fed on food containing 2 mg/ml BrdU for 8 h. In addition to the regular immunostaining protocol, testes were incubated for 30 min in 2 M HCl, neutralised with 100 mM borax solution and incubated with mouse anti-BrdU-Alexa 488 (BD Biosciences, 558599, 1:200) overnight.

Imaging and image analysis

Images were acquired using Leica SP5, Zeiss LSM700 and Zeiss LSM780 confocal microscopes with 40× or 63× water immersion objectives. Unless stated otherwise, images are single optical slices. Image quantifications were performed using Fiji (Schindelin et al., 2012), applying a double-blind protocol in appropriate cases. Image quantifications were tested for significance using Student's *t*-test or ANOVA followed by Tukey's Honest Significant Difference as appropriate. Images were prepared for publication using Adobe Photoshop and Illustrator.

Cell culture

S2 cells were cultivated in Schneider's Drosophila Medium (PAN-Biotech) with 10% FBS (Thermo Fisher Scientific) and transfected using calcium phosphate. The plasmids pMT-LT3-Dam, pMT-LT3-zfh1::Dam (Fig. S2), pUAST-Zfh1 act-DHFR tub-Gal4VP16 and pUAST-Zfh1-CIDm act-DHFR tub-Gal4VP16, respectively were generated by placing expression cassettes under the control of the metallothionein promoter of pmtn-HhN (Albert and Bökel, 2017). Sequences are provided in the Supplementary Information.

RNA-seq

Transgene expression from pMT-Zfh1 and pMT-Zfh1-CIDm was induced with 1 mM $CuSO_4$ for 24 h before RNA extraction using Direct-zol (Zymo Research). RNA was sequenced by the Center for Regenerative Therapies Dresden (CRTD)/Biotec (Dresden, Germany) NGS facility (Illumina HiSeq2000).

DamID

DNA was extracted from stable S2 cell lines transfected with pMT-LT3-Dam or pMT-LT3-zfh1::Dam without Cu^{2+} induction according to the protocol described in Vogel et al. (2007) omitting steps required for array hybridisation. DNA was extracted from testes proper as described in Laktionov et al. (2014). In brief, following 24 h induction at 30°C, hand-dissected testes from 50 zfh1::T2A::Gal4 tub-Gal80^{ts}/UAS-LT3-zfh1::Dam tub-Gal80^{ts} or zfh1::T2A::Gal4 tub-Gal80^{ts}/UAS-LT3-Dam tub-Gal80^{ts} males per replica were dissociated in 700 µl lysis buffer [0.1 M NaCl, 0.2 M sucrose, 0.1 M Tris-HCl (pH 9.1), 0.05 M EDTA and 0.5% SDS] by syringe aspiration, before overnight incubation at 56°C with 100 µg/ml dispase. Following RNase digestion and phenol/chloroform extraction, samples were processed according to Vogel et al. (2007) and sequenced by the CRTD/Biotec NGS facility (Illumina HiSeq2000).

Bioinformatics

NGS DamID reads were mapped to the *Drosophila* genome (dm6) using bowtie2 (Langmead and Salzberg, 2012). Peaks were called using DamID_seq analysis pipeline v1.4.2 (Marshall and Brand, 2015) and the find_peaks script (Marshall and Brand, 2015), with the false discovery rate threshold set to 0.01. Overlap of the Zfh1 DamID peaks with other sequence sets was analysed using the peakPermTest resampling/permutation approach implemented in the ChIPpeakAnno bioconductor package (Zhu et al., 2010), excluding the ENCODE *Drosophila* blacklist (Celniker et al., 2009). For each comparison, we performed 1000 resampling runs, artificially redistributing peaks and conserving their distribution of relative positions to landmarks of the respective associated genes (transcription starts and end, introns, and coding regions). Overlap between associated genes (defined as genes <1 kb distant from the ends of a Zfh1 DamID peak or other feature) was tested for significance using the χ^2-test. Enrichment of the degenerate, RCSI-like motif CTAATYRRNTT within Zfh1 DamID peaks was tested using PWMEnrich bioconductor.org/packages/release/bioc/html/PWMEnrich.html (doi:10.18129/B9.bioc.PWMEnrich)].

RNA-Seq analysis was performed using the DESeq R package (Anders and Huber, 2010). Reads were normalised according to the library complexity. Gene annotation was obtained from ENSEMBL (BDGP6 version) using the biomaRt R package (Smedley et al., 2009). Genes were flagged as significantly changing expression if the corresponding adjusted *P*-values were <0.05.

Acknowledgements

We thank the colleagues mentioned individually above, and the JEDI community for fly stocks, reagents and advice; the CRTD NGS sequencing facility for their support; Ilker Deniz for help with immunostainings; and Heiner Grandel, Christian Lange, Nikolay Ninov and Pavel Tomancak for discussions and critical reading of the manuscript.

Competing interests

The authors declare no competing or financial interests.

Author contributions

Conceptualization: C.B.; Methodology: E.A.A., N.V.T., C.B.; Formal analysis: E.A.A., O.A.P., N.V.T., C.B.; Investigation: E.A.A., O.A.P., A.L., C.B.; Resources: C.B.; Data curation: E.A.A., O.A.P., N.V.T.; Writing - original draft: C.B.; Writing - review & editing: C.B.; Supervision: C.B.; Project administration: C.B.; Funding acquisition: C.B.

Funding

The project was supported by a Zentrum für Regenerative Therapien Dresden (CRTD) seed grant, and a Deutsche Forschungsgemeinschaft grant (BO 3270/4-1) to C.B.

Data availability

DamID and RNA-seq results are presented in the supplementary information. The corresponding raw data files are available at the NCBI Sequence Read Archive (BioProject SRP150326).

Supplementary information

Supplementary information available online at
http://dev.biologists.org/lookup/doi/10.1242/dev.156315.supplemental

References

Albert, E. A. and Bökel, C. (2017). A cell based, high throughput assay for quantitative analysis of Hedgehog pathway activation using a Smoothened activation sensor. *Sci. Rep.* **7**, 14341.

Amoyel, M., Sanny, J., Burel, M. and Bach, E. A. (2013). Hedgehog is required for CySC self-renewal but does not contribute to the GSC niche in the *Drosophila* testis. *Development* **140**, 56-65.

Amoyel, M., Simons, B. D. and Bach, E. A. (2014). Neutral competition of stem cells is skewed by proliferative changes downstream of Hh and Hpo. *EMBO J.* **33**, 2295-2313.

Amoyel, M., Anderson, J., Suisse, A., Glasner, J. and Bach, E. A. (2016a). Socs36E controls niche competition by repressing MAPK signaling in the *Drosophila* testis. *PLoS Genet.* **12**, e1005815.

Amoyel, M., Hillion, K.-H., Margolis, S. R. and Bach, E. A. (2016b). Somatic stem cell differentiation is regulated by PI3K/Tor signaling in response to local cues. *Development* **143**, 3914-3925.

Anders, S. and Huber, W. (2010). Differential expression analysis for sequence count data. *Genome Biol.* **11**, R106.

Arnold, C. D., Gerlach, D., Stelzer, C., Boryn, L. M., Rath, M. and Stark, A. (2013). Genome-wide quantitative enhancer activity maps identified by STARR-seq. *Science* **339**, 1074-1077.

Baumgartner, R., Poernbacher, I., Buser, N., Hafen, E. and Stocker, H. (2010). The WW domain protein Kibra acts upstream of Hippo in *Drosophila*. *Dev. Cell* **18**, 309-316.

Beumer, J. and Clevers, H. (2016). Regulation and plasticity of intestinal stem cells during homeostasis and regeneration. *Development* **143**, 3639-3649.

Broihier, H. T., Moore, L. A., Van Doren, M., Newman, S. and Lehmann, R. (1998). *zfh-1* is required for germ cell migration and gonadal mesoderm development in *Drosophila*. *Development* **125**, 655-666.

Celniker, S. E., Dillon, L. A. L., Gerstein, M. B., Gunsalus, K. C., Henikoff, S., Karpen, G. H., Kellis, M., Lai, E. C., Lieb, J. D., MacAlpine, D. M. et al. (2009). Unlocking the secrets of the genome. *Nature* **459**, 927-930.

Chandel, N. S., Jasper, H., Ho, T. T. and Passegué, E. (2016). Metabolic regulation of stem cell function in tissue homeostasis and organismal ageing. *Nat. Cell Biol.* **18**, 823-832.

Chen, D. and McKearin, D. (2003). Dpp signaling silences *bam* transcription directly to establish asymmetric divisions of germline stem cells. *Curr. Biol.* **13**, 1786-1791.

Enderle, L. and McNeill, H. (2013). Hippo gains weight: added insights and complexity to pathway control. *Sci. Signal.* **6**, re7.

Fabrizio, J. J., Boyle, M. and DiNardo, S. (2003). A somatic role for *eyes absent* (*eya*) and *sine oculis* (*so*) in *Drosophila* spermatocyte development. *Dev. Biol.* **258**, 117-128.

Flaherty, M. S., Salis, P., Evans, C. J., Ekas, L. A., Marouf, A., Zavadil, J., Banerjee, U. and Bach, E. A. (2010). *chinmo* is a functional effector of the JAK/STAT pathway that regulates eye development, tumor formation, and stem cell self-renewal in *Drosophila*. *Dev. Cell* **18**, 556-568.

Fortini, M. E., Lai, Z. C. and Rubin, G. M. (1991). The *Drosophila zfh-1* and *zfh-2* genes encode novel proteins containing both zinc-finger and homeodomain motifs. *Mech. Dev.* **34**, 113-122.

Fuller, M. T. and Spradling, A. C. (2007). Male and female *Drosophila* germline stem cells: two versions of immortality. *Science* **316**, 402-404.

Genevet, A., Wehr, M. C., Brain, R., Thompson, B. J. and Tapon, N. (2010). Kibra is a regulator of the Salvador/Warts/Hippo signaling network. *Dev. Cell* **18**, 300-308.

Gheldof, A., Hulpiau, P., van Roy, F., De Craene, B. and Berx, G. (2012). Evolutionary functional analysis and molecular regulation of the ZEB transcription factors. *Cell. Mol. Life Sci.* **69**, 2527-2541.

Gratz, S. J., Ukken, F. P., Rubinstein, C. D., Thiede, G., Donohue, L. K., Cummings, A. M. and O'Connor-Giles, K. M. (2014). Highly specific and efficient CRISPR/Cas9-catalyzed homology-directed repair in *Drosophila*. *Genetics* **196**, 961-971.

Huang, J. and Kalderon, D. (2014). Coupling of Hedgehog and Hippo pathways promotes stem cell maintenance by stimulating proliferation. *J. Cell Biol.* **205**, 325-338.

Huang, J., Zhou, W., Watson, A. M., Jan, Y.-N. and Hong, Y. (2008). Efficient ends-out gene targeting in Drosophila. *Genetics* **180**, 703-707.

Hudson, A. G., Parrott, B. B., Qian, Y. and Schulz, C. (2013). A temporal signature of epidermal growth factor signaling regulates the differentiation of germline cells in testes of *Drosophila melanogaster*. *PLoS ONE* **8**, e70678.

Inaba, M., Buszczak, M. and Yamashita, Y. M. (2015). Nanotubes mediate niche-stem-cell signalling in the *Drosophila* testis. *Nature* **523**, 329-332.

Inaba, M., Sorenson, D. R., Kortus, M., Salzmann, V. and Yamashita, Y. M. (2017). Merlin is required for coordinating proliferation of two stem cell lineages in the *Drosophila* testis. *Sci. Rep.* **7**, 2502.

Irvine, K. D. and Harvey, K. F. (2015). Control of organ growth by patterning and Hippo signaling in *Drosophila*. *Cold Spring Harb. Perspect. Biol.* **7**, a019224.

Issigonis, M., Tulina, N., de Cuevas, M., Brawley, C., Sandler, L. and Matunis, E. (2009). JAK-STAT signal inhibition regulates competition in the *Drosophila* testis stem cell niche. *Science* **326**, 153-156.

Kawase, E., Wong, M. D., Ding, B. C. and Xie, T. (2004). Gbb/Bmp signaling is essential for maintaining germline stem cells and for repressing bam transcription in the *Drosophila* testis. *Development* **131**, 1365-1375.

Kiger, A. A., Jones, D. L., Schulz, C., Rogers, M. B. and Fuller, M. T. (2001). Stem cell self-renewal specified by JAK-STAT activation in response to a support cell cue. *Science* **294**, 2542-2545.

Lai, Z. C., Fortini, M. E. and Rubin, G. M. (1991). The embryonic expression patterns of *zfh-1* and *zfh-2*, two *Drosophila* genes encoding novel zinc-finger homeodomain proteins. *Mech. Dev.* **34**, 123-134.

Laktionov, P. P., White-Cooper, H., Maksimov, D. A. and Beliakin, S. N. (2014). Transcription factor comr acts as a direct activator in the genetic program controlling spermatogenesis in *D. melanogaster*. *Mol. Biol. (Mosk)* **48**, 153-165.

Langmead, B. and Salzberg, S. L. (2012). Fast gapped-read alignment with Bowtie 2. *Nat. Methods* **9**, 357-359.

Leatherman, J. L. and Dinardo, S. (2008). Zfh-1 controls somatic stem cell self-renewal in the *Drosophila* testis and nonautonomously influences germline stem cell self-renewal. *Cell Stem Cell* **3**, 44-54.

Leatherman, J. L. and Dinardo, S. (2010). Germline self-renewal requires cyst stem cells and stat regulates niche adhesion in *Drosophila* testes. *Nat. Cell Biol.* **12**, 806-811.

Le Bras, S. and Van Doren, M. (2006). Development of the male germline stem cell niche in *Drosophila*. *Dev. Biol.* **294**, 92-103.

Lee, T. and Luo, L. (1999). Mosaic analysis with a repressible cell marker for studies of gene function in neuronal morphogenesis. *Neuron* **22**, 451-461.

Losick, V. P., Morris, L. X., Fox, D. T. and Spradling, A. (2011). *Drosophila* stem cell niches: a decade of discovery suggests a unified view of stem cell regulation. *Dev. Cell* **21**, 159-171.

Ma, Q., Wawersik, M. and Matunis, E. L. (2014). The Jak-STAT target Chinmo prevents sex transformation of adult stem cells in the *Drosophila* testis niche. *Dev. Cell* **31**, 474-486.

Marshall, O. J. and Brand, A. H. (2015). damidseq_pipeline: an automated pipeline for processing DamID sequencing datasets. *Bioinformatics* **31**, 3371-3373.

Meng, Z., Moroishi, T. and Guan, K.-L. (2016). Mechanisms of Hippo pathway regulation. *Genes Dev.* **30**, 1-17.

Mi, H., Poudel, S., Muruganujan, A., Casagrande, J. T. and Thomas, P. D. (2016). PANTHER version 10: expanded protein families and functions, and analysis tools. *Nucleic Acids Res.* **44**, D336-D342.

Michel, M., Raabe, I., Kupinski, A. P., Pérez-Palencia, R. and Bökel, C. (2011). Local BMP receptor activation at adherens junctions in the *Drosophila* germline stem cell niche. *Nat. Commun.* **2**, 415.

Michel, M., Kupinski, A. P., Raabe, I. and Bokel, C. (2012). Hh signalling is essential for somatic stem cell maintenance in the *Drosophila* testis niche. *Development* **139**, 2663-2669.

Nègre, N., Brown, C. D., Ma, L., Bristow, C. A., Miller, S. W., Wagner, U., Kheradpour, P., Eaton, M. L., Loriaux, P., Sealfon, R. et al. (2011). A cis-regulatory map of the *Drosophila* genome. *Nature* **471**, 527-531.

Port, F., Chen, H.-M., Lee, T. and Bullock, S. L. (2014). Optimized CRISPR/Cas tools for efficient germline and somatic genome engineering in *Drosophila*. *Proc. Natl. Acad. Sci. USA* **111**, E2967-E2976.

Postigo, A. A. and Dean, D. C. (1999). ZEB represses transcription through interaction with the corepressor CtBP. *Proc. Natl. Acad. Sci. USA* **96**, 6683-6688.

Scadden, D. T. (2014). Nice neighborhood: emerging concepts of the stem cell niche. *Cell* **157**, 41-50.

Schindelin, J., Arganda-Carreras, I., Frise, E., Kaynig, V., Longair, M., Pietzsch, T., Preibisch, S., Rueden, C., Saalfeld, S., Schmid, B. et al. (2012). Fiji: an open-source platform for biological-image analysis. *Nat. Methods* **9**, 676-682.

Singh, S. R., Liu, Y., Zhao, J., Zeng, X. and Hou, S. X. (2016). The novel tumour suppressor Madm regulates stem cell competition in the *Drosophila* testis. *Nat. Commun.* **7**, 10473.

Smedley, D., Haider, S., Ballester, B., Holland, R., London, D., Thorisson, G. and Kasprzyk, A. (2009). BioMart – biological queries made easy. *BMC Genomics* **10**, 22.

Southall, T. D., Gold, K. S., Egger, B., Davidson, C. M., Caygill, E. E., Marshall, O. J. and Brand, A. H. (2013). Cell-type-specific profiling of gene expression and chromatin binding without cell isolation: assaying RNA Pol II occupancy in neural stem cells. *Dev. Cell* **26**, 101-112.

Su, M. T., Fujioka, M., Goto, T. and Bodmer, R. (1999). The *Drosophila* homeobox genes *zfh-1* and *even-skipped* are required for cardiac-specific differentiation of a numb-dependent lineage decision. *Development* **126**, 3241-3251.

Sun, S., Zhao, S. and Wang, Z. (2008). Genes of Hippo signaling network act unconventionally in the control of germline proliferation in *Drosophila*. *Dev. Dyn.* **237**, 270-275.

Szymczak, A. L., Workman, C. J., Wang, Y., Vignali, K. M., Dilioglou, S., Vanin, E. F. and Vignali, D. A. A. (2004). Correction of multi-gene deficiency in vivo using a single 'self-cleaving' 2A peptide-based retroviral vector. *Nat. Biotechnol.* **22**, 589-594.

Tapon, N., Harvey, K. F., Bell, D. W., Wahrer, D. C. R., Schiripo, T. A., Haber, D. and Hariharan, I. K. (2002). *salvador* Promotes both cell cycle exit and apoptosis in *Drosophila* and is mutated in human cancer cell lines. *Cell* **110**, 467-478.

Tulina, N. and Matunis, E. (2001). Control of stem cell self-renewal in *Drosophila* spermatogenesis by JAK-STAT signaling. *Science* **294**, 2546-2549.

Venken, K. J. T., Schulze, K. L., Haelterman, N. A., Pan, H., He, Y., Evans-Holm, M., Carlson, J. W., Levis, R. W., Spradling, A. C., Hoskins, R. A. et al. (2011). MiMIC: a highly versatile transposon insertion resource for engineering *Drosophila melanogaster* genes. *Nat. Methods* **8**, 737-743.

Vogel, M. J., Peric-Hupkes, D. and van Steensel, B. (2007). Detection of in vivo protein-DNA interactions using DamID in mammalian cells. *Nat. Protoc.* **2**, 1467-1478.

Xie, T. and Spradling, A. C. (2000). A niche maintaining germ line stem cells in the *Drosophila* ovary. *Science* **290**, 328-330.

Yu, J., Zheng, Y., Dong, J., Klusza, S., Deng, W.-M. and Pan, D. (2010). Kibra functions as a tumor suppressor protein that regulates Hippo signaling in conjunction with Merlin and Expanded. *Dev. Cell* **18**, 288-299.

Zhang, L., Ren, F., Zhang, Q., Chen, Y., Wang, B. and Jiang, J. (2008). The TEAD/TEF family of transcription factor Scalloped mediates Hippo signaling in organ size control. *Dev. Cell* **14**, 377-387.

Zhu, L. J., Gazin, C., Lawson, N. D., Pagès, H., Lin, S. M., Lapointe, D. S. and Green, M. R. (2010). ChIPpeakAnno: a Bioconductor package to annotate ChIP-seq and ChIP-chip data. *BMC Bioinformatics* **11**, 237.

Supplementary Information

Table S1: Zfh1 DamID peaks and associated genes from S2 cells

Click here to Download Table S1

Table S2: Transcripts with altered expression levels in S2 cells overexpressing Zfh1-CIDm vs. Zfh1

Click here to Download Table S2

Table S3: Zfh1 DamID peaks and associated genes from CySCs

Click here to Download Table S3

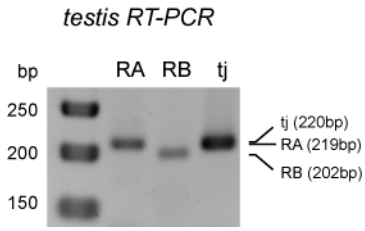

Figure S1 - Expression of Zfh1 isoforms

RT-PCR on adult testis mRNA extracts reveals expression of both Zfh1-RA and -RB isoforms. tj, expression control.

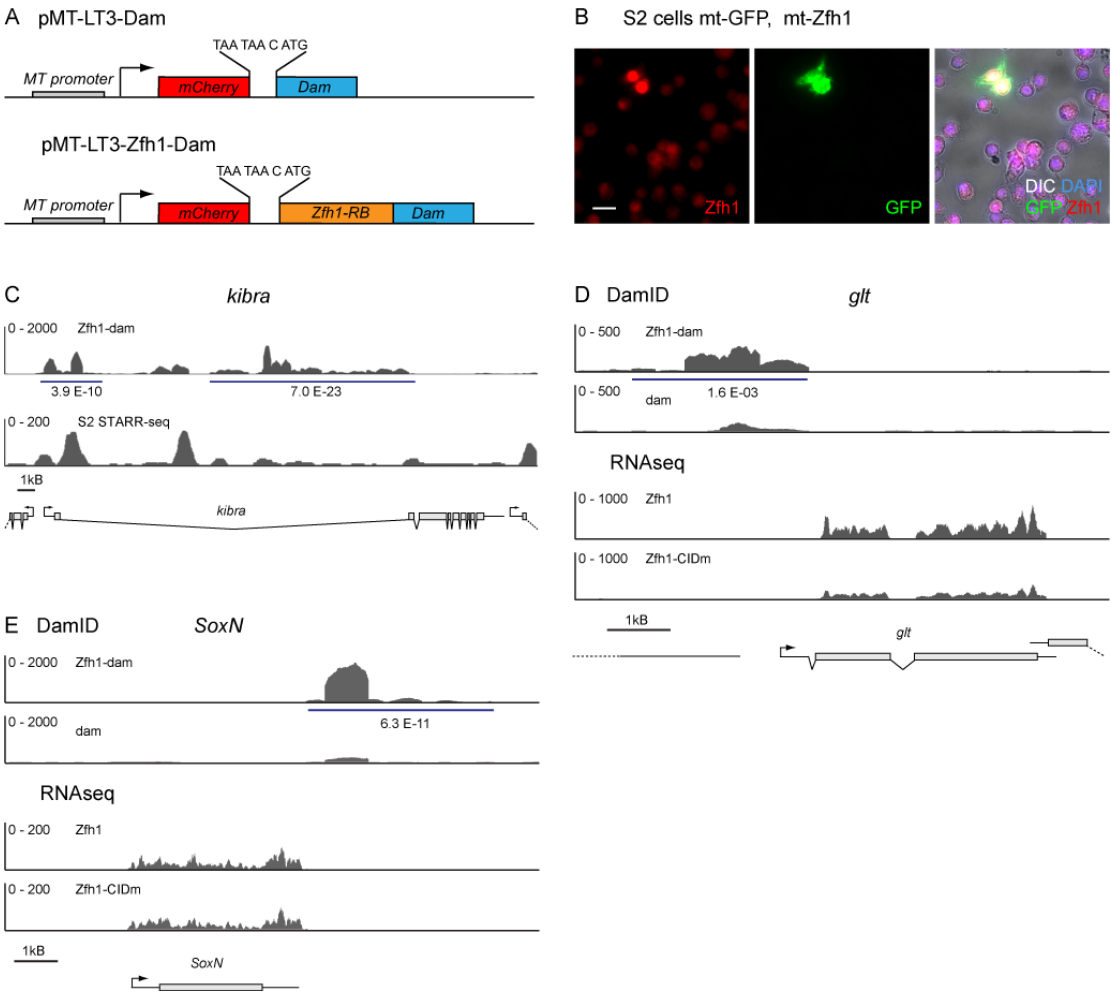

Figure S2 - Zfh1 in S2 cells

A Schematic representation of the DamID vectors used for stable transfection. Levels of Dam and the Zfh1-Dam fusion protein are minimized by the presence of an mCherry leader ORF termed LT3 followed by two stop codons and a frame shift that limits expression to rare transcriptional reinitiation events.

B S2 cells transiently cotransfected with plasmids expressing either Zfh1 or GFP under control of the metallothionein (mt) promoter. Following a 24h induction, strong Zfh1 immunostaining (red) is visible in GFP positive (green) nuclei, while a weaker, endogenous Zfh1 signal can also be seen in the nontransfected cells. Nuclei marked by DAPI (blue), cell outlines by DIC (grayscale).

C One of the two DamID peaks identified at the *kibra* locus that is localized near the transcriptional start site overlaps with a transcriptional activator region identified by STARR-seq.

D The *glt* gene is associated with a single, 5´ localized Zfh1 DamID peak and exhibits reduced transcription following overexpression of the Zfh1-CIDm construct unable to bind the CtBP transcriptional corepressor.

E The *SoxN* gene is associated with a single, 3´ localized Zfh1 DamID peak but does not exhibit any change in transcription following Zfh1-CIDm overexpression.

Peaks called by damid_seq marked by blue line; FDR indicated.

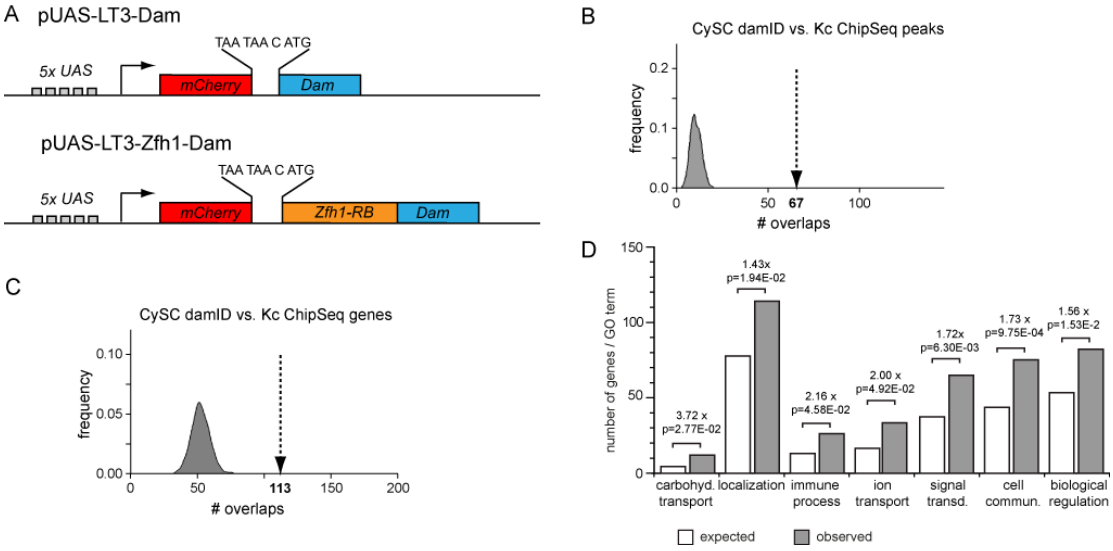

Figure S3 - Zfh1 DamID in S2 cells

A Schematic representation of the DamID vectors used for UAS/Gal4 driven expression in the CySCs. Levels of Dam and the Zfh1-Dam fusion protein are again minimized by the presence of an mCherry leader ORF termed LT3 followed by two stop codons and a frame shift.

B Zfh1 DamID peaks in CySCs significantly colocalize with Zfh1 ChIP peaks in Kc167 cells ($p<0.001$, permutation test). Distribution of overlaps from 1000 resamplings plotted against frequency; dashed arrow indicates observed overlap.

C Same as **B** for the respective associated genes (DamID peak falling within transcript region ± 1kB, $p<0.001$, χ^2-test).

D GO-slim terms overrepresented for genes associated with at least one Zfh1 DamID peak in CySCs. Expected and observed numbers of genes, enrichment factor, and p-value given for terms exhibiting significant overrepresentation.

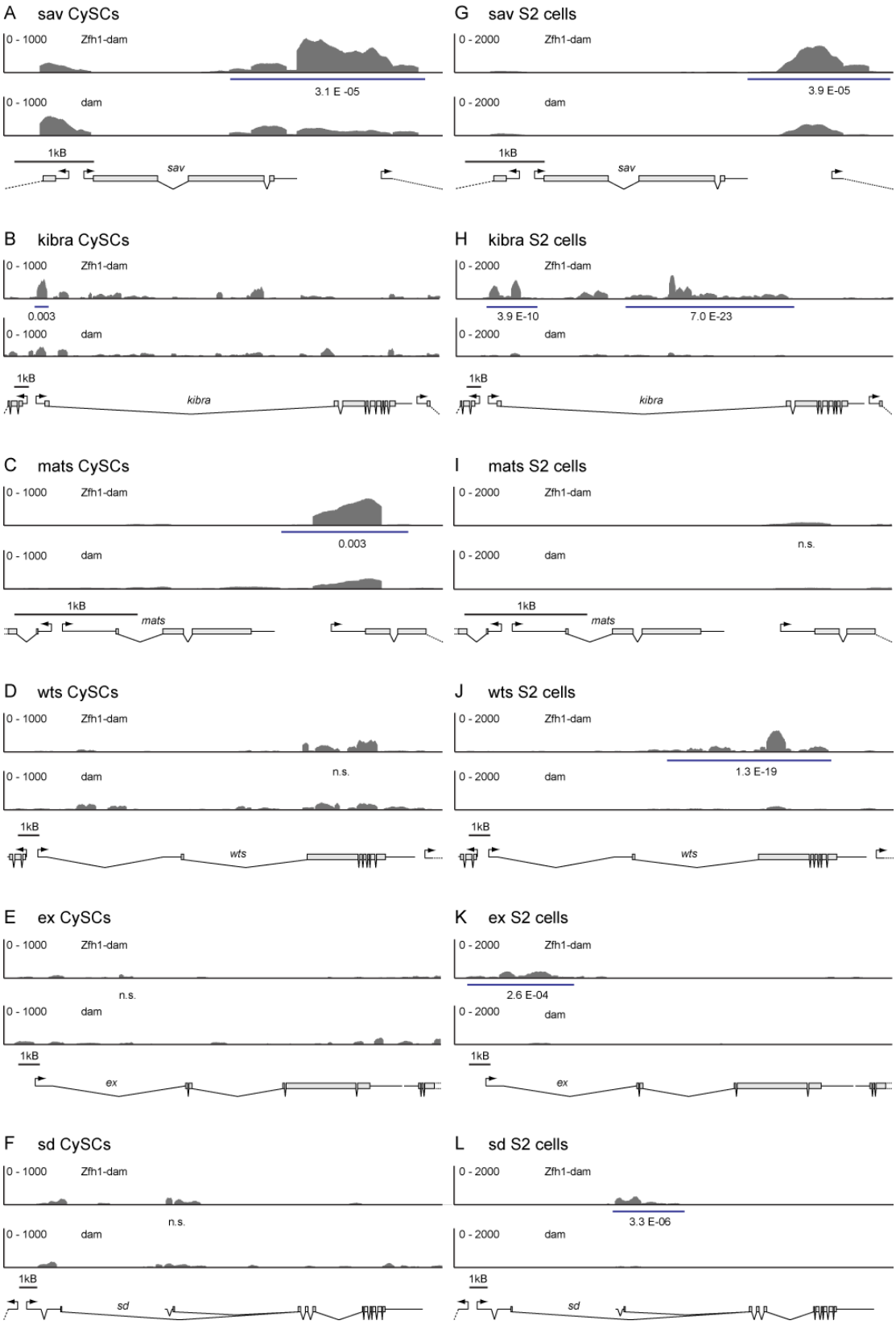

Figure S4 - Zfh1 DamID peaks near Hippo pathway components

A-E NGS reads from Zfh1-Dam (top panel) and Dam only control samples (bottom) panels for selected components of the Hippo pathway reveals Zfh1 binding peaks in CySCs.

G-K Same for S2 cells.

DamID peaks as called by damid_seq, blue line; FDR indicated.

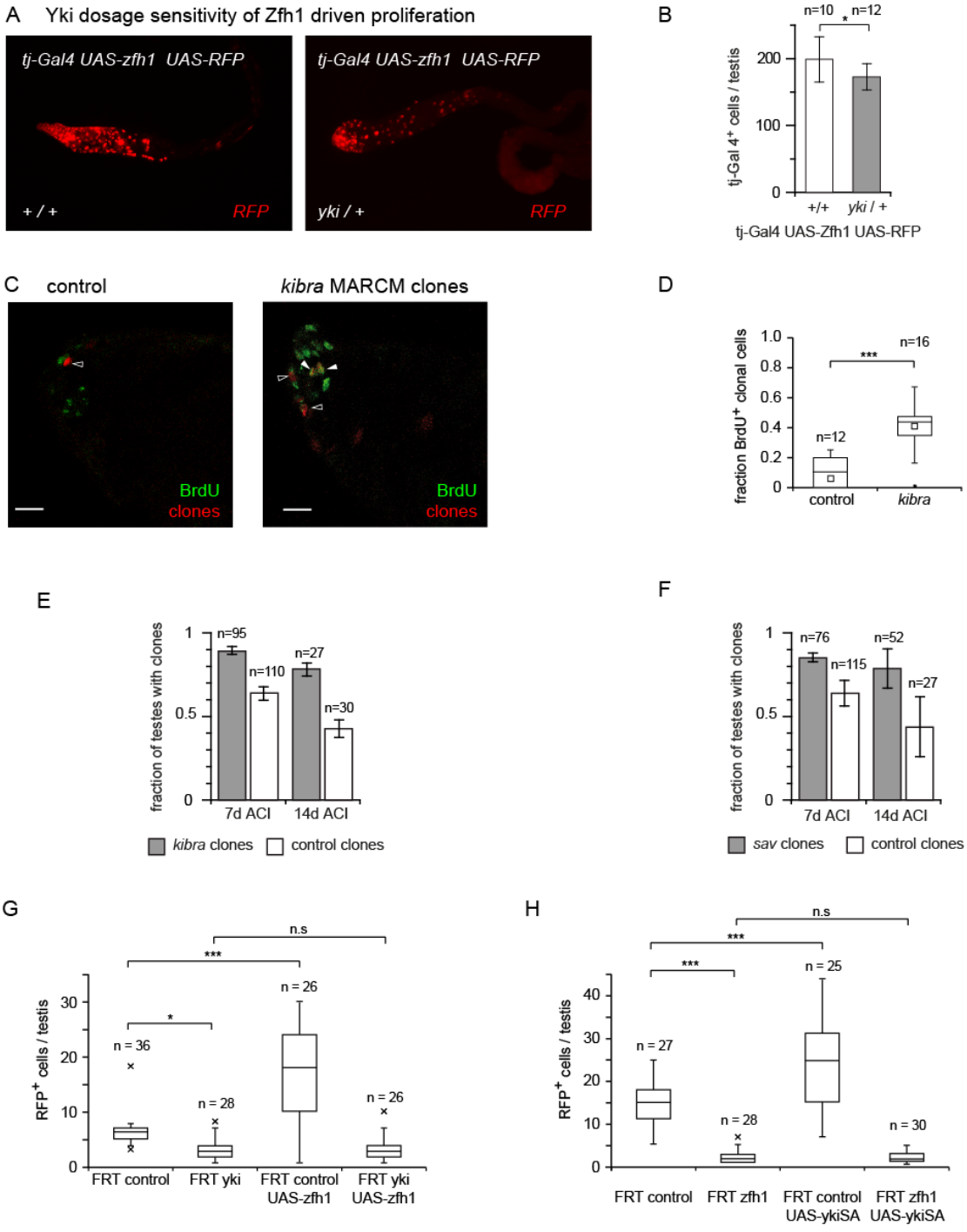

Figure S5 - Hippo signalling and CySC maintenance and proliferation

A Overexpression of UAS-Zfh1 under Tj-Gal4 control for five days causes expansion of somatic cells as visualized by co-overexpression of UAS-nlsRFP.

B Quantification of the RFP positive nuclei reveals a 14% reduction in number when one copy of *yki* is removed.

C Following an 8h pulse of BrdU feeding, *kibra* MARCM clones (RFP, red) contained a larger fraction of BrdU (green) positive cells than corresponding, neutral control clones.

D Quantification of the fraction of BrdU positive cells relative to the total number of cells per clone.

E Compared with control clones, which are gradually lost over time, homozygous *kibra* clones are retained in a larger fraction of testes one or two weeks ACI.

F Same as **E** for homozygous *sav* and control clones.

G,H Epistasis analysis for Yki and Zfh1. **G,** Loss of Yki reduces clone size (as reflected by the number of RFP positive cells per testis). This cannot be rescued by clonal overexpression of Zfh1, even though this is in control clones sufficient to increase the number of marked cells. **H**, Overexpression of activated, nonphosphorylatable Yki can conversely not rescue the loss of RFP positive cells homozygous mutant for *zfh1* even though it is sufficient to expand control clones.

Scale bars, 10μm. **B,E,F**: Columns indicate mean, error bars standard deviation **D,G,H**: Box indicates first and third quartile and median. Whiskers indicate data range up to 1.5x interquartile distance. Outliers marked individually. *, $p<0.05$; ***, $p<0.001$ (**B**,**D**: t-test, **G,H**: Anova); n, number of testes.

Plasmid sequences

Annotated sequences for the following plasmids are provided in genbank flat (.gb) format:

pRK2-zfh1_GFP

pRK2-zfh1_T2A_Gal4

pBSKS-attB kibra exon 5-9

pattB-sav_T2A_GFPnls

pattB -sav-ATG_GFPnls full

pattB -sav-ATG_GFPnls ΔNsiPst

pattB -sav-ATG_GFPnls ΔRCSI

pUAST-LT3-Zfh1::Dam

pMT-LT3-Dam

pMT-LT3-zfh1::Dam

pMT-zfh1-eGFP

pMT-zfh1-CIDm-eGFP

Click here to Download the plasmid sequences